This is an open access article published under an ACS AuthorChoice License, which permits copying and redistribution of the article or any adaptations for non-commercial purposes.

ACS AUTHORCHOICE

ACS OMEGA

http://pubs.acs.org/journal/acsodf

Article

Phase Diagram Study of Sodium Dodecyl Sulfate Using Dissipative Particle Dynamics

Monika Choudhary and S. M. Kamil*

Cite This: *ACS Omega* 2020, 5, 22891−22900

Read Online

ACCESS | Metrics & More | Article Recommendations

ABSTRACT: Dissipative particle dynamics (DPD) simulations are performed to study the phase transition of sodium dodecyl sulfate (SDS) in aqueous solution, which is an anionic surfactant commonly known as sodium dodecyl sulfate. In this work, the aim is to find a coarse-grained minimal model suitable to produce the full phase diagram of SDS. We examine the coarse-grained models of SDS, which have been used in earlier computational studies to produce the phases as well as for finding the critical micelle concentration (CMC) of SDS. We contrast the results based on these models with the experimental observations to assess their accuracy. Our research also takes into account the importance of sodium ions, which come from the partial dissociation of SDS, when dissolved in water. The effect of sodium ion has not been considered explicitly in the computational work done so far using dissipative particle dynamics. In light of the above explorations, we propose new models for SDS and demonstrate that they successfully produce a compendious SDS phase diagram, which can precisely overlay the experimental results.

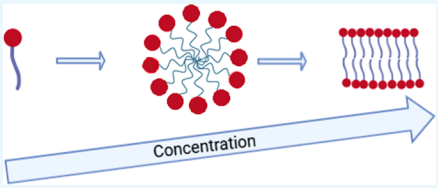

Downloaded via 157.44.170.100 on May 15, 2021 at 09:14:38 (UTC).
See https://pubs.acs.org/sharingguidelines for options on how to legitimately share published articles.

1. INTRODUCTION

Surfactants are chemical substances that consist of hydrophobic and hydrophilic parts. The amphiphilic nature of these compounds results in a plethora of useful applications. Surfactants are frequently used in domestic and industrial applications like cleaning, hygiene, cosmetic, personal care products, fibers, textiles, paints, plastics, pharmaceuticals, food products, petroleum, etc. Sodium dodecyl sulfate (SDS) is an anionic surfactant. Its chemical formula is given by $CH_3(CH_2)_{11}SO_4Na$. It consists of a chain of 12 carbon atoms attached to a sulfate group. The polar head group SO_4 and a hydrocarbon tail give amphiphilic properties to this synthetic organic compound. When added to water, SDS has a tendency to form different self-assemblies with change in concentration. They can form micelles above a certain concentration called critical micelle concentration (CMC).[1] SDS has been extensively used in the above-mentioned examples due to its low cost and easy availability. SDS shows many interesting properties when mixed with other surfactants. Thus, it is of much interest for industry and science alike to develop a better understanding of its assemblies and how it varies with different thermodynamic parameters.[2] The phase diagrams of many amphiphilic systems have been explored using experimental methods.[2−4] However, the experiments have their own constraints and sometimes the results can only provide a brief idea about complexities of the system and its evolution in time. In contrast, computational methods serve as a very powerful and efficient means to study complex structures at various levels. In the computational approach, once there is a standard model for a given system, it becomes way easier to explore complexities of the system in the presence of other chemical substances without actually performing the corresponding experiments.

In the list of computational methods, molecular dynamics (MD) is an earmarked simulation method. However, performing molecular dynamics for the self-assembling process is very much demanding in terms of memory and time. For instance, CMCs are of the order of 10^{-5}−10^{-3} M, where M stands for mole per liter. To simulate such a system with such a concentration, we need to have particles of the order of 10^7, which is way too large for computational approaches like molecular dynamics (MD).[5−11] When it is required to simulate the process on a large scale, especially when one is considerate with time scales relevant to phenomena akin to the formation of membranes, etc., methods like mesoscale models are used.[12−19] However, with a coarse grain technique, such as dissipative particle dynamics (DPD), the complexity of the system can be significantly reduced. We can work for a larger system with a simplified model, retaining a reasonable accuracy of the result. In DPD, the clusters of atoms, within a molecule, are replaced by appropriate single units, called beads. These beads are subjected to conservative, dissipative, and random forces as per the model. The time evolution is calculated using Newton's equation of motion. The preference of DPD over

Received: May 14, 2020
Accepted: August 19, 2020
Published: September 2, 2020

© 2020 American Chemical Society

https://dx.doi.org/10.1021/acsomega.0c02255
ACS Omega 2020, 5, 22891−22900

other coarse grain techniques relies on the simplicity and reproducibility of different complex phases in soft matter. The DPD technique was first proposed by Hoogerbrugge and Koelman[20] in 1992 and was first implemented by Groot and Madden in 1998[21] to study block copolymers. Since then DPD has been applied to a wide variety of soft matter problems.[20−26] Ample computational studies using DPD have been carried out to understand the CMC behavior of SDS.[30,31] However, the complete phase diagram of SDS is yet to be produced using computational techniques.

The experimental phase diagram of SDS was obtained by Kekicheff et al., and it was published long back in 1988.[32] Our paper is focused on two objectives: first, to investigate the efficacy of all of the SDS models available in the existing literature, and second, try to produce the full phase diagram of SDS using the DPD technique. In our literature survey, we came across broadly two types of papers, which are related to SDS or the mixture of SDS with other amphiphilic surfactants and ionic salts.[34] The first type of papers focus on CMC behavior of SDS,[30,31] while the second type of papers aim to produce phases of mixture of SDS with other surfactants. To the best of our knowledge, no one except Kim et al.[36] has attempted to produce the full phase diagram of SDS. Unfortunately, the results presented therein do not agree with the true experimental phase diagram. A few groups have tried to obtain CMC of the sodium dodecyl sulfate and have been successful to some extent. For instance, in 2006, Wu et al.[37] obtained the CMC of SDS using DPD. Their results are qualitatively close to the experimentally obtained results. However, this paper did not include the rigidity in the simulation model, the importance of which has been emphasized in later publications.[39] In a subsequent work by Mai et al. in 2014,[30] a CMC of 9.020 mmol/L was obtained, which is in close agreement with the experimentally obtained value. In their work, two distinct features were included in the model: first, the effect of rigidity, and second, the effect of electrostatic interaction, which was included implicitly. In 2015, Mao et al.[31] included the effect of electrostatic interaction using smeared charged distribution in the DPD model, giving a different CMC. Some papers reported the simulation of surface tension of SDS using DPD.[40]

The remaining of this paper is organized as follows. In Section 1, a succinct idea of SDS and need for SDS modeling has been given. In Section II, simulation details are thoroughly elucidated. In Section III, various models mentioned in the literature are examined, and in Section IV, some new models of SDS are proposed and the relevant interaction parameters are fixed wherever it is required based on the meticulous study done so far. Section V enlists all of the simulation results. In Section VI, a brief summary of the research is given, which is further concluded with future perspectives.

II. SIMULATION DETAILS

Dissipative particle dynamics (DPD) is a coarse grain technique particularly designed for simulating the hydrodynamic behavior of a given system. DPD is a particle-based technique in which atoms and molecules are lumped together as DPD beads, where the number of atoms packed together in a lump is known as coarse-graining parameter and is usually represented by N_m. This lumping into DPD beads is an important feature of this technique as it plays a major role in computational speedup. It is similar to the molecular dynamics simulation, but with this technique, it is possible to analyze complex phenomena such as self-assembly of the surfactants, which is not feasible with classical methods due to limited time and length scales. DPD gives rise to decreased degrees of freedom, which enables one to analyze complex systems at a bigger time and length scales, thus making it computationally efficient and cheaper. The approach is straightforward, as it starts with Newton's second law, which is the first step in molecular dynamics also. But unlike conventional molecular dynamics, here, the net force acting between beads i and j, separated at a distance $r_{ij} = |\boldsymbol{r}_i - \boldsymbol{r}_j|$ and relative velocity $\boldsymbol{v}_{ij} = \boldsymbol{v}_i - \boldsymbol{v}_j$, consists of three components: conservative ($\boldsymbol{F}_{ij}^{C}$), dissipative ($\boldsymbol{F}_{ij}^{D}$), and random ($\boldsymbol{F}_{ij}^{R}$) forces.[24] The total force $\boldsymbol{F}_{ij}^{DPD}$ can be written as the sum of the three forces mentioned above

$$\boldsymbol{F}_i^{DPD} = \sum_{i \neq j} (\boldsymbol{F}_{ij}^{C} + \boldsymbol{F}_{ij}^{D} + \boldsymbol{F}_{ij}^{R}) \tag{1}$$

where the constituent forces are of the form,

$$\boldsymbol{F}_{ij}^{C} = \begin{cases} a_{ij}(1 - r_{ij}/r_c)\hat{\boldsymbol{r}}_{ij} & \text{if } r_{ij} < r_c, \\ 0 & \text{if } \quad r_{ij} > r_c \end{cases} \tag{2}$$

$$\boldsymbol{F}_{ij}^{D} = -\gamma\omega^{D}(r_{ij})(\hat{\boldsymbol{r}}_{ij}\cdot\boldsymbol{v}_{ij})\hat{\boldsymbol{r}}_{ij} \tag{3}$$

$$\boldsymbol{F}_{ij}^{R} = \sigma\omega^{R}(r_{ij})\, \theta_{ij}\, \Delta t^{-1/2}\, \hat{\boldsymbol{r}}_{ij} \tag{4}$$

where a_{ij} is the maximum repulsive conservative force between particles i and j, γ is the friction coefficient in dissipative force, and σ is the noise amplitude in random force. The weight $\omega^{D}(r_{ij})$ can be chosen arbitrarily, but it should satisfy the following relation

$$\omega^{D}(r_{ij}) = [\omega^{R}(r_{ij})]^2 \tag{5}$$

and

$$\sigma^2 = 2\gamma k_B T \tag{6}$$

where k_B is the Boltzmann constant. A simple choice for the weight function is given by

$$\omega^{D}(r_{ij}) = \begin{cases} (1 - r_{ij})^2 & \text{if } r < r_c, \\ 0 & \text{if } r \geq r_c \end{cases} \tag{7}$$

In this paper, only reduced units have been used. The mass is given by m for all of the particles, and the unit of length is r_c, i.e., the cutoff value. While studying the system, we have kept $\sigma = 3$ and $k_B T = 1$, which gives $\gamma = 4.5$ from eq 6.[24] The timestep, Δt, is kept to be 0.03 τ (τ is the time unit). Lammps[28] was used to integrate Newton's equations of motion using the Shardlow algorithm.[41] For bonding between particles of surfactant, we have used a harmonic spring force given by $\boldsymbol{F}_{ij} = C(r_{ij} - r_o)\hat{r}_{ij}$, where C is the spring constant and has a value equal to 4 and r_o is set to zero.[27]

Rigidity is introduced by controlling the potential energy U_{ijk}^{B} associated with each bonding angle in the molecule, viz.

$$U_{ijk}^{B} = \frac{1}{2}k_\theta(\theta_{ijk} - \theta_o)^2 \tag{8}$$

where k_θ represents the bending angle force constant, θ_{ijk} is the angle between bonds ij and jk, and θ_o represents the equilibrium bending angle. We have used $k_\theta = 6$ and $\theta_o = \pi$ in our simulation.

https://dx.doi.org/10.1021/acsomega.0c02255
ACS Omega 2020, 5, 22891−22900

ρ_{DPD} is the number of beads per unit volume in simulation units. Every bead assumes the volume of approximately three water molecules, which is equal to 90 Å^3 at room temperature. ρ_{DPD} is chosen such that $\rho_{DPD}\, r_c^3 = 3$, and thus the volume of r_c^3 has a net physical volume equivalent to 270 Å^3, which leads to the radius of interaction r_c = 6.46 Å. The size of the simulation box used in our simulation is 20 × 20 × 20, and the number density is set to ρ_{DPD} = 3, giving a total of 24 000 DPD beads. Periodic boundary conditions and NVT ensemble were adopted. The simulations were also performed for a box size of 30 × 30 × 30 at 45 and 80 wt % (model V) so as to find out the effect of box size on our simulation results. However, we did not find any significant difference between the outcomes of the two. In this work, 25 × 10^5 DPD steps were carried out.

The computing time was long enough for the system to achieve an equilibrium state (see Figure 1). The simulation results were tested for different initial states.

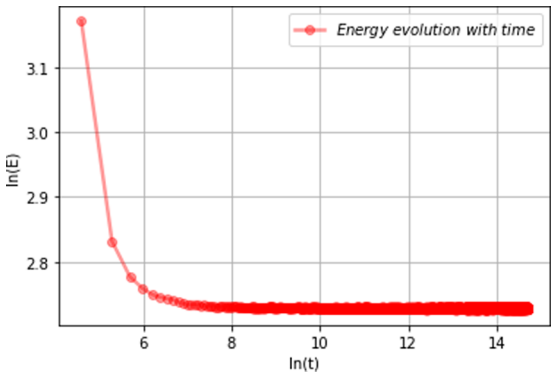

Figure 1. Ln−ln plot of the variation of total energy with time for model II at 60 wt % of SDS.

The pivotal parameter for performing DPD simulation is a_{ij}. According to Groot and Warren,[24] the interaction parameters a_{ij}, between same type of beads is derived from the compressibility of liquid, which is given by

$$a_{ij} = \frac{16N_m - 1}{0.2}\frac{k_B T}{\rho_{DPD}} = \alpha \tag{9}$$

where N_m is the number of water molecules coarsened in one bead. For different types of beads, we have

$$a_{ij} = \alpha + \frac{1}{0.231}\chi_{ij} \tag{10}$$

where χ_{ij} is the Flory−Huggins parameter. From eq 9, for N_m = 3, α is set to 78. For different types of particles i and j, χ_{ij} can be obtained by estimating the mixing energy between two molecular entities

$$\chi_{ij} = z\left(\frac{E_{ij} - \frac{1}{2}(E_{ii} + E_{jj})}{RT}\right) \tag{11}$$

where z is the coordination number, E_{ij} is the mixing energy of a particular ij pair, R is the ideal gas constant, and T is the temperature. The Flory−Huggins parameters for eq 10 can be obtained from the research work done by Chen et al.[29] Monte Carlo simulation can be performed to compute the mixing free energy of two kinds of substances from their pair contact energies. The computed average mixing energies then leads to evaluation of the Flory−Huggins parameter, χ_{ij}. However, the DPD parameters that have been used in the current research are derived from χ_{ij}, which is directly taken from Mai et al.[30] The set of χ_{ij} values is given in Table 1, with H and T representing head and tail in the models adopted for SDS (see Section III). One may note that, to account for increased repulsion between ionized beads, the repulsion parameter (a_{ii}) between the ionized beads has been changed from 78 to 86.7. We have chosen the same value in our simulations following Mai et al., and a detailed analysis can be found in the citation.[30]

Table 1. Bead−Bead Repulsion Parameter taken from Mai et al.[30]

Bead−Bead	χ_{ij}	a_{ij}
H−H	2	86.7
H−T	1.5−10.5	84−124
H−W	−3 to −0.5	65−75.8
T−T	0	78
T−W	2.7−6	90−104
W−W	0	78

III. COMPARATIVE STUDY OF VARIOUS MODELS

To establish a model that can produce a phase diagram of SDS, it is necessary to go through the experimental work centrally based on SDS. In that sequence, the first accountable experimental work was done by Reiss-Husson and Luzzati.[45] According to this work, spherical micelles for SDS appear at 0.07 weight fraction, sphere-to-rod transition appears around 0.25 weight fraction, and on further increasing the weight fraction to 0.40, more complex phases appear.[36,45] Another calorimetric study was done by Fontell in 1981[46] and Kekicheff et al. in 1988.[32] A sketch of the phase diagram, obtained with these references is drawn in Figure 2. This figure gives a coarse idea of the actual phase diagram, and the actual phase diagram could be seen in the publication by Kekicheff et al. in 1988.[32]

Hitherto, many researchers have attempted to work on SDS with several objectives. The most commonly used computational technique has been molecular dynamics. However,

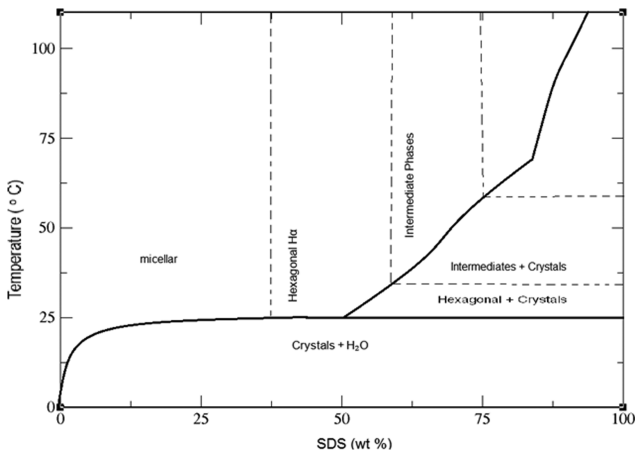

Figure 2. Schematic phase diagram of SDS (sodium dodecyl sulfate) and water drawn after studying experimental papers by Fontell[46] and Kekicheff et al.[32] This diagram only gives a coarse idea about the phases of SDS. For details on the actual phase diagram of SDS, refer to the above-mentioned research papers. Reprinted in part with permission from the reference number [32].[32] Copyright [1989] Elsevier.

https://dx.doi.org/10.1021/acsomega.0c02255
ACS Omega 2020, 5, 22891−22900

molecular dynamics has its limitations when it comes to complex fluids due to time and length scales and majorly because of the interaction potential used between the atom or molecules. Despite all constraints, in 1990, a research paper based on molecular dynamics simulation of SDS was reported by Shelley, Watanabe, and Klein.[5] It involved a 182 ps simulation of a 42-monomer SDS micelle. In 1995, a 120 ps simulation of a 60-monomer SDS micelle was performed.[47] Again, due to the limitations of length and time scales, it was computationally difficult to extend it to larger systems. However, with DPD, it is possible to perform the simulation for a bigger system. As it gives us the advantage of soft potential with which computational cost can be significantly reduced, in 2005, a DPD simulation was performed for SDS solution by Kim, Byun, and Kwak.[36] In this simulation, the coarse grain model that was adapted for SDS was H1T4 (where H in H1T4 represents the head of the SDS surfactant, whereas T represents the tail part of SDS). The effect of Na ion was incorporated by coarse graining it with water. It was found in this work[36] that the simulation results were dependent upon the initial condition. Moreover, the results obtained therein were not similar to the experimentally obtained results (even qualitatively). In this league, a few more models of SDS were explored as discussed in Section 1. In 2006, Wu et al.[37] also used the H1T4 model for SDS with different interaction parameters a_{ij}. The CMC obtained by Wu et al. using the H1T4 model was $1.7 \pm 0.2 \times 10^{-4}$ in mole fraction. However, there was no physical basis provided for the interaction parameters that were used in the paper. In 2009, one more study was done for determining the CMC of SDS by Duan et al.[38] by relating CMC with the interaction between water and tail beads. However, the scheme of varying the interaction between tail and the water bead was not accurate.

In 2014, Li et al.[35] published a paper for a catanionic system consisting of SDS and DTAB. We extracted the relevant parameters from this paper[35] for SDS and performed the simulations to check phases of SDS formed at different concentrations. Unfortunately, it did not emerge as a potential model for SDS surfactant as phases obtained with the extracted parameters were not at all similar to the experimental phases. To continue our study, the simulation model for SDS as given by Mai et al.[30] was investigated. This was preferred among all of the models discussed so far because their CMC results were closest to the experimentally obtained results.[48,49] However, we found that at higher concentrations, it could not produce the experimentally obtained phases of SDS. From the above discussion, it can be concluded that there is no single set of interaction parameters in the literature that can reproduce the full phase diagram of SDS. In the subsequent year, one more study was conducted by Mao et al.[31] by taking explicit electrostatic interaction into consideration. However, if we want to make the model simple and proceed without bringing any additional explicit force in picture, such as electrostatic interaction between the ions as done in the previous paper, then we have to come up with a scheme that can account for the effect of ions present in the solution. This could be done in two ways, either we need to consider the impact of ionic nature of surfactants implicitly or we need to incorporate the sodium-ion bead explicitly in the modeling scheme. Due to the reversible reaction of the counterions with the parent body, we took the association parameter into account[42−44] in a coarse-grained model of the system of SDS. According to ref 42, a part of SDS dissociates into sodium ions and ionized surfactants. A theoretical result in support of the above conclusion was also found,[33] which emphasizes the point of micellar dissociation too. Considering all of the aspects of SDS models discussed in this section, we propose new models for SDS, with an aim to cover all of the facets of SDS without adding any additional potential. A thorough description of the models, which we have considered for our research, are given in the subsequent section.

IV. SDS MODELS USED IN OUR SIMULATION

In our investigation, we realized that unfortunately no model mentioned in the existing literature[30,31,36,37,39,40] can fully describe the experimentally obtained phase diagram. Thus, it was required to build a better model, which can produce all the experimentally obtained phases. Aided with the knowledge acquired from the existing literature, we propose seven new models for SDS, which put emphasis on various aspects of the SDS properties required to be undertaken for coarse-graining the system. To simulate the effect of counterions in the aqueous solution of SDS, we need to consider the dissociation of SDS, viz.

$$CH_3(CH_2)_{11}SO_4Na \rightleftharpoons CH_3(CH_2)_{11}SO_4^- + Na^+ \quad (12)$$

This is a reversible chemical reaction, and depending on the chemical equilibrium, the solution will involve a mixture of undissociated SDS molecules ($CH_3(CH_2)_{11}SO_4Na$) as well as dissociated ions. In principle, we must tune the interaction between $CH_3(CH_2)_{11}SO_4^-$ and Na^+ so that it will balance the required dissociated and undissociated molecules of SDS. In the first attempt, we want to avoid this tuning of the reaction kinetics and want to see the effect of mixing of dissociated and undissociated molecules of SDS on the equilibrium phases of SDS in water. In Figure 3, we depict the DPD coarse-graining scheme that has been adopted for our investigation. In this scheme, three water molecules and one sodium ion are considered to form a single bead, which is denoted by WNa,

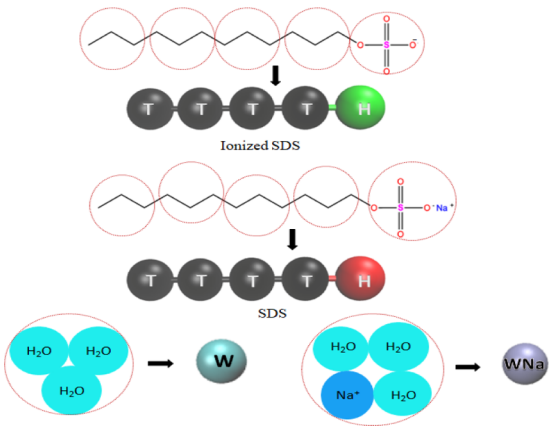

Figure 3. Coarse grain model for SDS used in our simulation. Sodium dodecyl sulfate (SDS) is expressed as H1T4, where H and T represent the head and tail parts of SDS, respectively. Here, SDS is expressed in two forms; 1. Ionic SDS (Na ion dissociated from the rest of SDS) represented as H in green and T in black, 2. Unionized SDS (Na ion intact) is represented as H in red and T in black. In the model, three water molecules are lumped together to form a single water bead and the dissociated counterion Na that comes from ionized SDS (head shown in green) is lumped with three water molecules to form a single WNa bead. Ionic SDS is denoted by SDS(D), and unionized SDS is denoted simply by SDS.

https://dx.doi.org/10.1021/acsomega.0c02255
ACS Omega 2020, 5, 22891−22900

whereas three water molecules constituting one DPD bead is denoted by W. Coarse-grained SDS molecule is modeled in two forms, one with charged head H(SDS(D)), and another with uncharged head H(SDS) depending on whether the SDS is ionized or not. SDS(D) represents the sodium dodecyl sulfate, from which Na ion has been dissociated. As explained further in the caption of Figure 3, coarse-grained model for SDS used in our simulation is expressed as H1T4, where H and T represent the head and tail parts of SDS, respectively. Here, SDS is expressed in two forms: (i) ionic SDS (Na ion dissociated from the rest of SDS) represented as H in green and T in black, and (ii) SDS (Na-ion intact) represented as H in red and T in black. In the model, three water molecules are lumped together to form a single water bead W and the dissociated counterion Na that comes from ionized SDS (head shown in green) is lumped with three water molecules to form a single WNa bead. Note that ionic SDS is denoted by SDS(D) and unionized SDS is denoted simply by SDS. To have a clear idea about our approach, it is necessary to have a look at the models given in Figure 4, for which simulations were

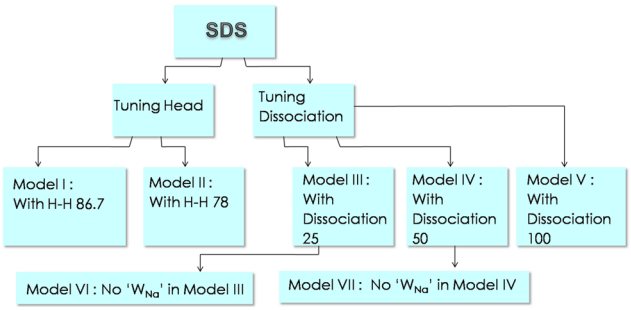

Figure 4. Classification of all of the models that have been shaped and used in our simulation study of SDS. This classification primarily deals with two classes: 1. Considering the tuning of H−H interaction parameter (model I and model II) and 2. Considering the dissociation of SDS surfactants into ions. Model III involves dissociated surfactants SDS(D) and undissociated SDS surfactants in the ratio of 25:75, and the dissociated sodium ions Na^+ are incorporated with water beads, which is further explained in Figure 5. Similarly, 50% of SDS surfactants are dissociated in model IV and the corresponding dissociated sodium ions Na^+ are clubbed with water beads accordingly. Model V contains 100% of SDS surfactants dissociated (SDS(D)), and corresponding dissociated sodium ions are clubbed with W beads changing them into WNa beads. In this manner, model II involves 0% of SDS surfactant dissociated. Model VI and model VII are derived from model III and model IV by ignoring the dissociated sodium ions. Model I can be considered the same as model V (100% dissociation of SDS) but ignoring the inclusion of dissociated sodium ions.

performed. We work for seven models in this research by incorporating the coarse grain scheme that has been just discussed. As shown in Figure 4, we classify the models into two categories, tuning head, where the interaction parameters between heads (H−H) were tuned with values a_{ij} = 86.7 (model I) and a_{ij} = 78 (model II), and tuning dissociation, where dissociation of SDS has been varied from 0 to 100, considering the dissociation of SDS surfactants into ions. Model III involves dissociated surfactants SDS(D) and undissociated SDS surfactants in a ratio of 25:75, and the dissociated sodium ions Na^+ are incorporated with water beads, which is further explained in Figure 5. Similarly, 50% of SDS surfactants are dissociated in model IV and the

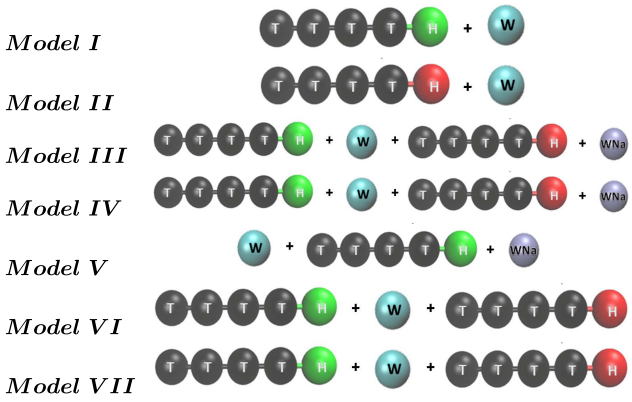

Figure 5. Schematic categorizing various beads, which have been used in different models. It shows a one-to-one correspondence of the model and beads.

corresponding dissociated sodium ions Na^+ are clubbed with water beads accordingly. Model V contains 100% of SDS surfactant dissociated (SDS(D)), and the corresponding dissociated sodium ions are clubbed with W beads changing them into WNa beads. In this manner, model II is 0% dissociated. Model VI and model VII are derived from model III and model IV by ignoring the dissociated sodium ions. Model I can be considered the same as model V (100% dissociation of SDS) but ignoring the inclusion of dissociated sodium ions. The repulsion parameters used in this simulation are listed in Table 2. One may note that, to account for

Table 2. Interaction Parameters α_{ij} Used in DPD Simulations of SDS for the Proposed Models[a]

	H(SDS)	H(SDS(D))	T(SDS)	W	WNa
H(SDS)	78	78	104	65	65
H(SDS(D))	78	86.7	104	65	60
T(SDS)	104	104	78	93.5	93.5
W	65	65	93.5	78	78
WNa	65	60	93.5	78	86.7

[a]Note that ionic SDS is denoted as SDS(D) and unionized SDS is denoted simply as SDS, as explained in Figure 3. H(SDS) denotes head bead associated with unionized surfactant, H(SDS(D)) is the head bead associated with ionized surfactant, W denotes a bead containing three water molecules, and the bead denoted by WNa contains three water molecules and a sodium ion Na^+.

increased repulsion between ionized beads, the repulsion parameter (a_{ii}) between the ionized beads has been changed from 78 to 86.7. We have chosen this value following Mai et al.,[30] wherein a detailed analysis can be found.

V. RESULTS AND DISCUSSION

After going through refs 30, 31, 36, 37, 39, 40 that were mentioned in the previous sections, a set of models were developed for SDS by describing minute details wherever possible. These simulations were carried out at room temperature (27° C).

V.I. Self-Assembly of the SDS System. Simulations were performed at various concentrations for all of the classes of models as discussed above and are depicted in Figure 4. As a result of this study, a variety of self-assemblies were obtained, which are listed in Table 3. Comparing the results given in Table 3 with the experimental phase diagram given in Figure 2,

https://dx.doi.org/10.1021/acsomega.0c02255
ACS Omega 2020, 5, 22891−22900

Table 3. Phases Obtained as a Result of Simulation of Various Models of SDS at Different Concentrations[a]

SDS (wt %)	model I	model II	model III	model IV	model V	model VI	model VII
25	micelles	micelles	micelles	micelles	micelles	micelles	micelles
30	micelles	micelles	micelles	micelles	micelles	micelles	micelles
35	micelles + rods	micelles + rods	micelles	micelles	micelles	micelles	micelles + rods
38	micelles + rods	micelles + rods	micelles + rods	micelles + rods	micelles + rods	micelles + rods	micelles + rods
40	micelles + rods	micelles + rods	rods	micelles + rods	micelles + rods	rods	micelles + rods
42	hexagonal	micelles + rods	rods	micelles + rods	rods	rods	hexagonal
45	hexagonal	hexagonal	hexagonal	interwoven rods	hexagonal	hexagonal	hexagonal
48	hexagonal	hexagonal	hexagonal	hexagonal	hexagonal	hexagonal	hexagonal
50	hexagonal	hexagonal(S)	hexagonal	interwoven rods	hexagonal	interwoven rods	interwoven rods
52	rods	hexagonal(S)	hexagonal	interwoven rods	hexagonal	hexagonal	hexagonal
55	rods	hexagonal(S)	hexagonal	hexagonal	hexagonal	hexagonal(S)	interwoven rods
58	interwoven rods	rods	interwoven rods	hexagonal	hexagonal	interwoven rods	interwoven rods
60	interwoven rods	interwoven rods	rods	interwoven rods	hexagonal	hexagonal	interwoven rods
75	rhombohedral	lamellar	lamellar	lamellar	lamellar	rhombohedral	lamellar
80	lamellar	lamellar	lamellar	lamellar	lamellar	lamellar	lamellar

[a]Micelles refers to the spherical micelles, rods to the cylindrical micelles, hexagonal to the hexagonal columnar phase, hexagonal(S) to the hexagonal columnar phase formed by not so straight rods, where S stands for swirly, interwoven rods to the merged rods, rhombohedral to the bicontinuous rhombohedral form formed by the tail part, lamellar to the layers stacks of SDS, respectively.

it is clear that for all of the models, simulation results are matching qualitatively with the experimental result. However, we could see a minor difference in the onset of phases. For instance, for model I, we could find the onset of hexagonal phase at 45 wt % of SDS; for model II, it starts at 42 wt %; for model III, at 45 wt %; for model IV, at 48 wt %; and for model V, at 45 wt %. Model V gives the closest match with the experimental phase diagram in our simulations. With some models, we could find the bicontinuous forms. In the beginning, it was assumed that they are not the stable forms and with increment in simulation run, a discrete phase would be obtained. However, it persisted even when the simulation time was doubled.

Model I and model V differ from each other only by the presence of sodium ions. Comparing the phases of model I and model V in Table 3, we find that at concentration 52 wt %, the hexagonal phase is not stable in model I. It starts to differ from model V, which consistently shows hexagonal phase up to 60 wt %. At 75 wt %, model I assumes the rhombohedral phase, whereas model V shows lamellar phase. Interestingly, model VI also shows rhombohedral phase and model VII shows lamellar phase. In construction, model VI is close to model V, whereas model VII is close to model I. Model III and model VI differ by the presence of sodium ions; here, again, we see model III preferring stable hexagonal phase. Model IV and model VII also differ by the presence of sodium ions, but in this case, we could not say anything conclusively. Overall, it seems that the addition of sodium ions provides more order and the system prefers hexagonal phase. Model II shows bend or swirly hexagonal and differs from model I in head–head interaction. It seems that the increased value of head interaction prefers a more straight and rigid hexagonal phase.

Formation of self-assembly is also determined by the interaction between the aggregates formed, which causes transition to ordered "mesophase" structures. At this level, we are not including any explicit long-range interaction. However, DPD preserves the hydrodynamic interactions, which is a long-range interaction. At lower concentrations, say above CMC, but less than 40 wt % of SDS (in DPD units), we got micelles of SDS. It is shown in Figure 6. Initially, when the concentration of SDS is less, the surfactants self-assemble

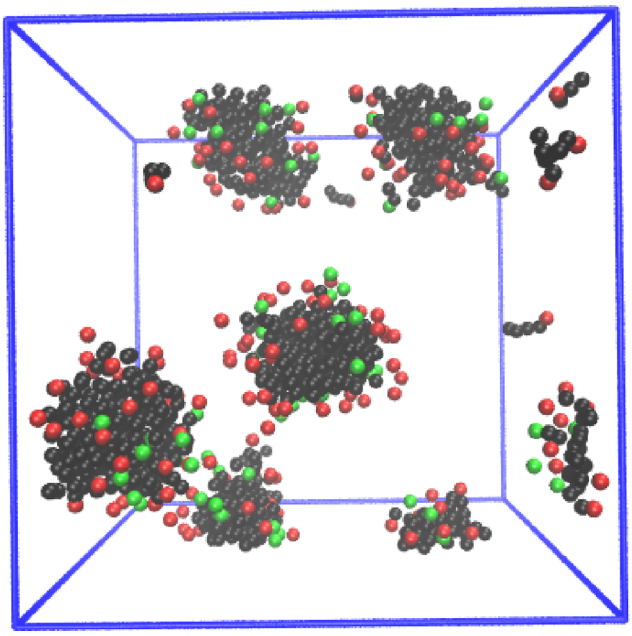

Figure 6. Micelle formation at 5 wt %. The color scheme used is as in Figure 3. This simulation is done for model III.

into micelles to minimize the contact of hydrophobic part, i.e., the tail with water, as shown in Figure 7 at 25 wt %. On further increasing the concentration of SDS, we observed a change of phase at 45 wt %, from spherical to rodlike structures, as shown in Figure 8. Therefore, at higher surfactant concentrations, spherical micelles transform into rodlike structures. On further increasing the concentration, it remains at the rodlike micelle, as shown in Figure 9.

Our simulations show that at higher concentrations, these rods align to form a hexagonal columnar phase, as shown in Figure 10a. To obtain the information on the aggregate shape, we plotted the radial distribution function $g(r)$ in Figures 10b and 11. In Figure 10b, we plot radial distribution function $g(r)$, between heads of SDS, and in Figure 11a, we plot the RDF between head and tail of SDS for model III at 45 wt %. In Figure 11b, we plot the distribution of sodium ions around the

https://dx.doi.org/10.1021/acsomega.0c02255
ACS Omega 2020, 5, 22891−22900

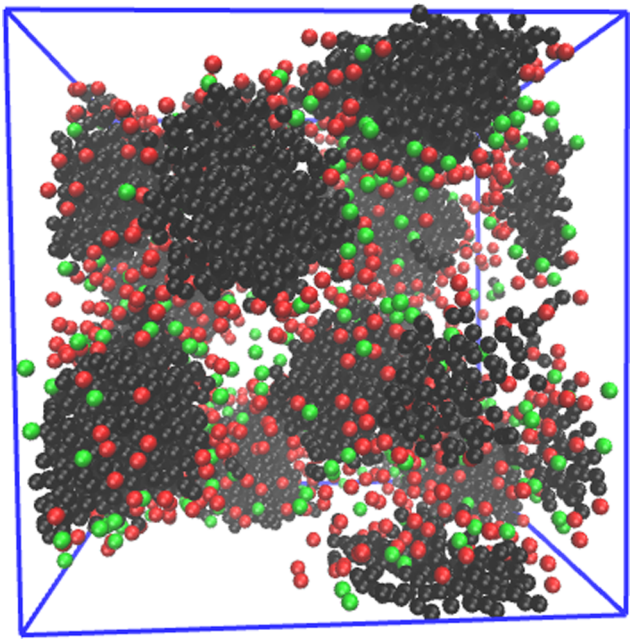

Figure 7. Micelle formation at 25 wt %. The color scheme used is as in Figure 3. This simulation is done for model III.

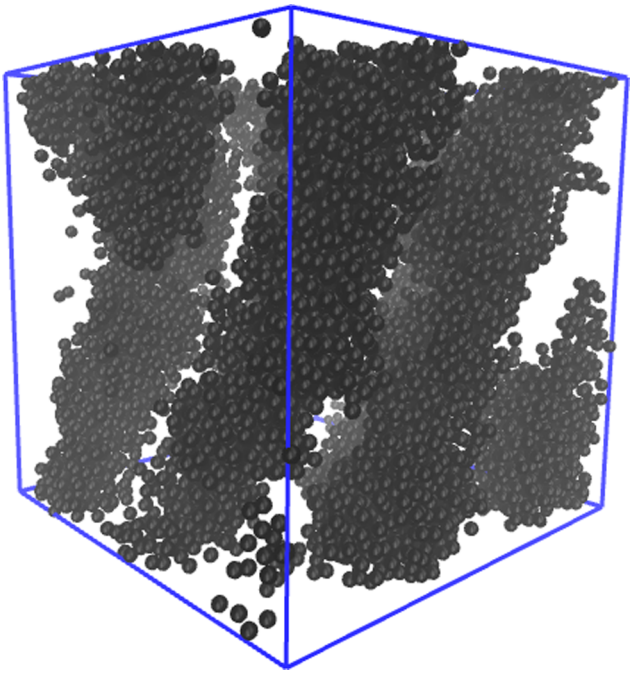

Figure 9. Simulation result simulated at 45 wt %. For clarity, we have shown the tail (in black) part only. The self-assembly obtained here is still hexagonal. Again, this simulation result has been performed for model III.

cylinders of SDS. For plotting the sodium-ion distribution around cylinders, we actually calculated the radial distribution function between last tail bead and sodium ions. Figure 12 shows how SDS evolves with an increase in concentration for a given temperature. Figure 12b,d,f gives a virtual idea of how the self-assembly would look like at the given concentration. However, Figure 12a,c,e shows the result of the performed simulation. For clarity, only the tail part (black) is shown in Figure 12b. Here, a general trend was observed in all models, i.e., the transition from micelle to rod and then to hexagonal form (other forms were obtained too, which are enlisted in Table 3). Figure 13 shows how the total average energy of the system varies with concentration, and hence, it can be concluded that the average energy increases linearly with an increase in the concentration of SDS in water. All of the models show the same trend; however, model IV and model V show low energy at high concentration because of the presence of sodium ions. The attractive interaction among sodium ions and heads of the micelles results in reduction in the total energy.

As a part of our investigation, CMC for all of the models discussed above was also calculated. The estimated result is given in Table 4. The CMC obtained with all of the models in our simulations was in close agreement with the experimentally obtained result, which is 8.2×10^{-3} mol/L obtained by electrical conductivity method.[48,49] This serves as a validation for the models proposed by us for SDS.

VI. CONCLUSION AND FUTURE PERSPECTIVE

In this work, our key goal was to design a DPD model of SDS that can provide a fundamental understanding of the SDS system. In this search, various models were studied and benchmarked.[30,31,36,37,39,40] It was anticipated that the available

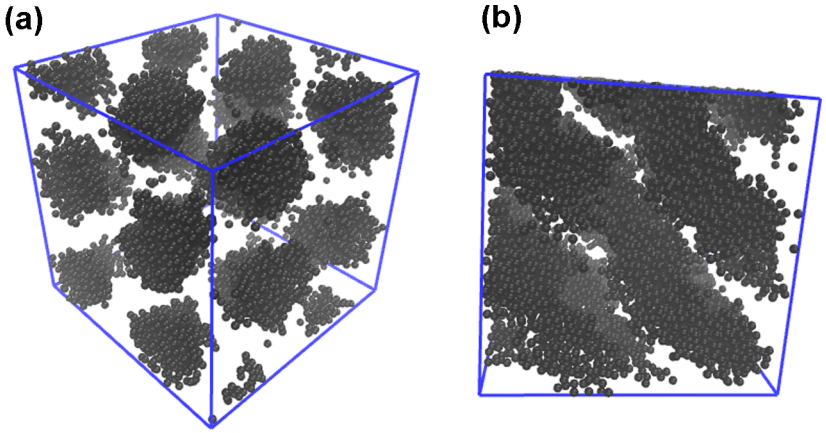

Figure 8. Hexagonal phase at 45 wt %. (a) Top view and (b) side view of the rod phase. For clarity, we have shown the tail (in black) part only. This simulation result is for model III.

https://dx.doi.org/10.1021/acsomega.0c02255
ACS Omega 2020, 5, 22891−22900

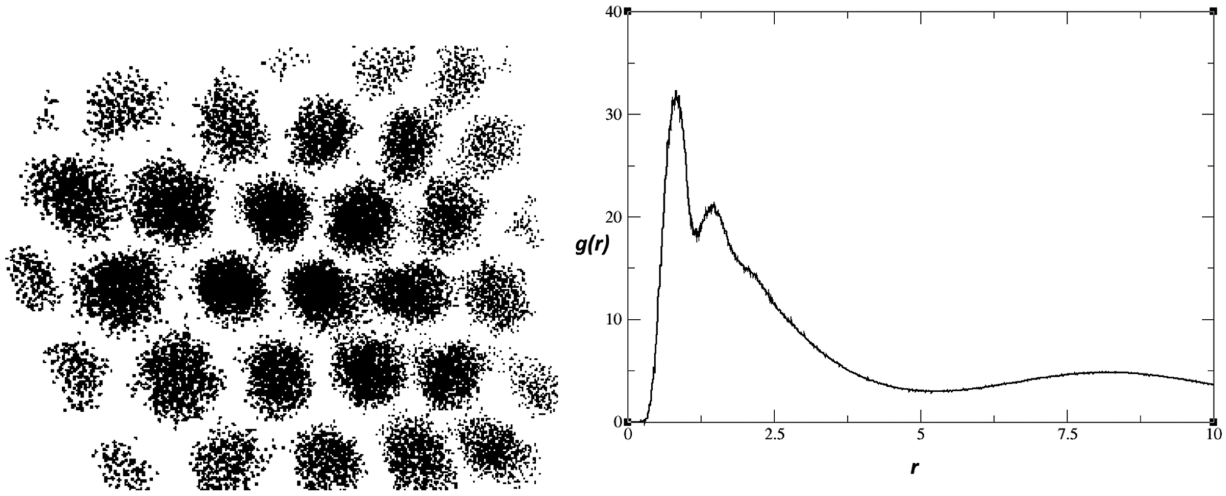

(a) (b)

Figure 10. (a) Cross section of the simulated result for model III at 45 wt % of SDS, which forms a hexagonal structure. (b) Radial distribution function between the beads of heads at 45 wt % of SDS for model III.

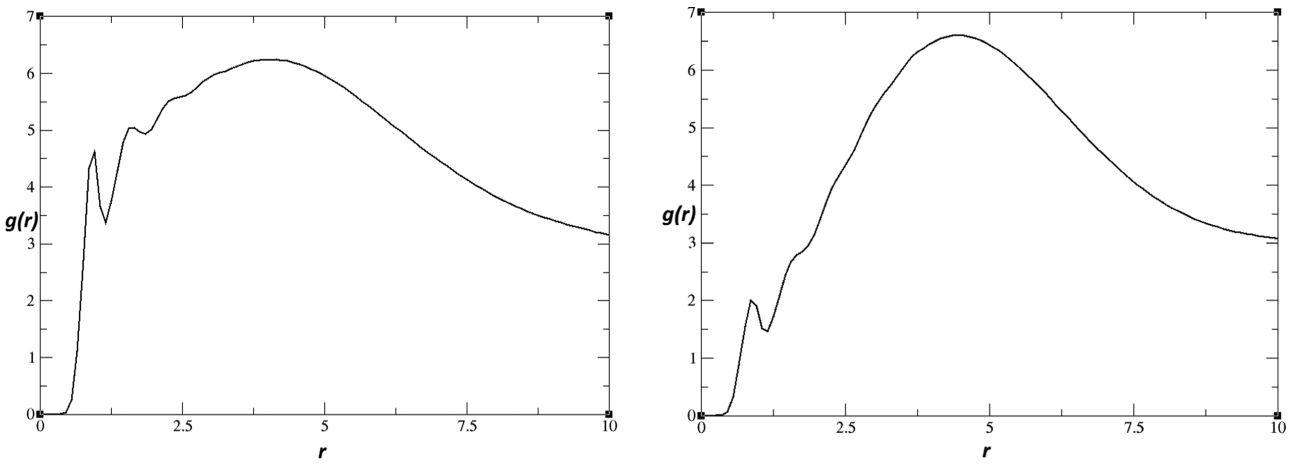

(a) (b)

Figure 11. (a) Radial distribution function $g(r)$ as a function of the distance between head and tail of SDS for model III at 45 wt % of SDS. (b) Distribution of sodium ion around cylindrical micelles for model III for 45 wt %.

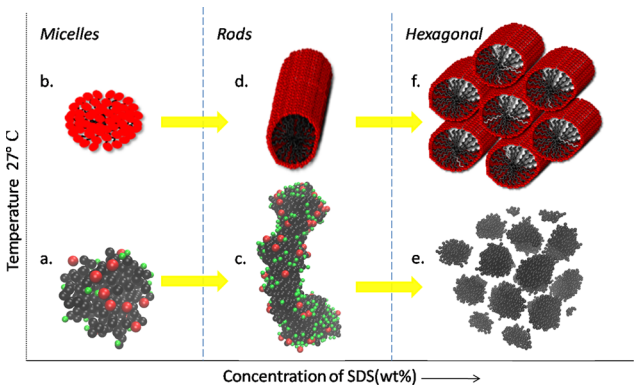

Figure 12. Schematic of the evolution of SDS phases with increase in concentration at 27 °C. (b, d, f) Phases obtained as a result of simulation. (a, c, e) Actual simulation result. (e) The tail part is shown for clarity.

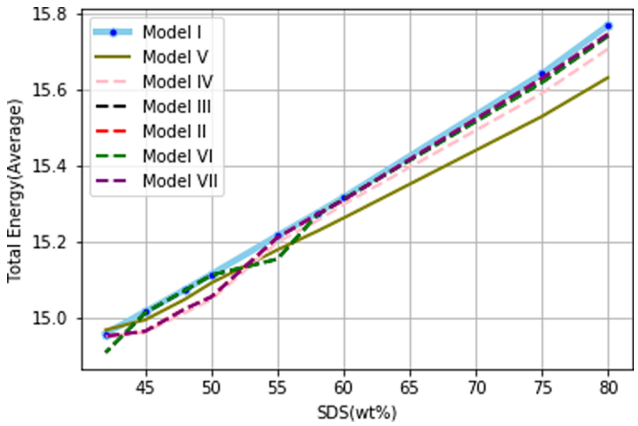

Figure 13. Variation of average of energy with concentration of SDS in water.

models for SDS would give some insight for the system of SDS and water, and with some minimal modification, we would achieve our goal. It was observed that when we performed the simulations using the SDS models available in the literature, they could not produce the expected phase diagram. We

https://dx.doi.org/10.1021/acsomega.0c02255
ACS Omega 2020, 5, 22891−22900

Table 4. CMC Obtained as a Result of Simulation for Various Models

s.no.	model	CMC (mol/L)
1.	model I	6.9×10^{-3}
2.	model II	6.59×10^{-3}
3.	model III	6.299×10^{-3}
4.	model IV	6.064×10^{-3}
5.	model V	6.970×10^{-3}
6.	model VI	6.5946×10^{-3}
7.	model VII	6.958×10^{-3}

attributed these deviations to the parameter values considered in the earlier works, due to which a major portion of the experimental phase diagram could not be produced. To establish adequate models for SDS, we checked the efficacy of the force parameters for SDS that have been used in earlier works.[30,31,36,37,39,40] It was perceived that the models for SDS, existing in the literature, were efficient for finding CMC only and a very few were good up to certain concentrations. To achieve the various phases at different concentrations, either one has to change the parameters of the DPD model or bring additional degrees of freedom by introducing charges as done in ref 31. This modification of force parameters becomes necessary due to various chemical changes at different concentrations. We proposed that the SDS can be modeled by measuring the influence of each attribute like H−H interaction or Na-ion contribution. Accordingly, we came up with seven candidate models. Analysis of the simulation results of these models shed some light on the effect of dissociation, inclusion of sodium ions, and head−head interaction. Model II and model V with the current values of interaction parameters produce qualitatively a major part of SDS phase diagrams in sequence as they appear in experiment. We found that model V is the best among all, as it is able to yield results very close to experimental observation. However, it will require further fine tuning to make agreement even better. Rest of the models also produce a major part of the phase diagram, but other phases also appear in-between, which are different from experimental results. Inclusion of sodium ions reduces the total energy of the system, as shown in the graph depicted in Figure 13. The present study was done at room temperature. In the near future, we aim to extend this model for higher temperatures as well. Investigation of kinematical aspects will also be of interest.

AUTHOR INFORMATION

Corresponding Author

S. M. Kamil − *Department of Physics, Shiv Nadar University, Greater Noida, Uttar Pradesh 201314, India;* orcid.org/0000-0003-4266-5281; Email: kamil.syed@snu.edu.in

Author

Monika Choudhary − *Department of Physics, Shiv Nadar University, Greater Noida, Uttar Pradesh 201314, India*

Complete contact information is available at: https://pubs.acs.org/10.1021/acsomega.0c02255

Notes

The authors declare no competing financial interest.

ACKNOWLEDGMENTS

The authors thank Dr. Santosh Kumar for his kind help and useful inputs. They are also grateful to Shiv Nadar University for providing the computational facility.

REFERENCES

(1) Israelachvili, J. N. *Intermolecular and Surface Forces*, 3rd ed.; Academic Press: San Diego, 2011; p 512.

(2) Tanford, C. *Hydrophobic Effect*, 2nd ed.; Wiley: New York, 1980.

(3) Larson, R. G. *The Structure and Rheology of Complex Fluids*, Oxford University Press: New York, 1999.

(4) Schramm, L. L.; Stasiuk, E. N.; Marangoni, D. G. Surfactant and their applications. *Annu. Rep. Prog. Chem., Sect. C: Phys. Chem.* **2003**, *99*, 3−48.

(5) Shelley, J.; Watanabe, K.; Klein, M. L. Simulation of sodium dodecyl sulphate. *Int. J. Quatum Chem.* **1990**, *38*, 103−117.

(6) Ryjkina, E.; Kuhn, H.; Rehage, H.; Müller, F.; Peggau, J. Molecular Dynamic Computer Simulations of Phase Behavior of Non-Ionic Surfactants. *Angew. Chem., Int. Ed.* **2002**, *41*, 983−986.

(7) Marrink, S. J.; Tieleman, D. P.; Menk, A. E. Molecular Dynamics Simulation of the Kinetics of Spontaneous. *J. Phys. Chem. B* **2000**, *104*, 12165−12173.

(8) Bruce, C. D.; Berkowitz, M. L.; Perera, L.; Forbes, M. D. E. Molecular Dynamics Simulation of Sodium Dodecyl Sulfate Micelle in Water: Micellar Structural Characteristics and Counterion Distribution. *J. Phys. Chem. B* **2002**, *106*, 3788−3793.

(9) Sammalkorpi, M.; Karttunen, M.; Haataja, M. Structural Properties of Ionic Detergent Aggregates: A Large-Scale Molecular Dynamics Study of Sodium Dodecyl Sulfate. *J. Phys. Chem. B* **2007**, *111*, 11722−11733.

(10) Ben-Naim, A.; Stillinger, F. H. Critical micelle concentration and the size distribution of surfactant aggregates. *J. Phys. Chem. A.* **1980**, *84*, 2872−2876.

(11) Alasiri, H. Determining Critical Micelle Concentrations of Surfactants Based on Viscosity Calculations from Coarse-Grained Molecular Dynamics Simulations. *Energy Fuels* **2019**, *33*, 2408−2412.

(12) Ramakrishnan, N.; Kumar, P. B. S.; Radhakrishnan, R. Mesoscale computational studies of membrane bilayer remodeling by curvature-inducing proteins. *Phys. Rep.* **2014**, *543*, 1−60.

(13) Marrink, S. J.; Corradi, V.; Souza, P. C. T.; Ingólfsson, H. I.; Tieleman, D. P.; Sansom, M. S. P. Computational Modeling of Realistic Cell Membranes. *Chem. Rev.* **2019**, *119*, 6184−6226.

(14) Ruiz-Morales, Y.; Romero-Martínez, A. Coarse-Grain Molecular Dynamics Simulations To Investigate the Bulk Viscosity and Critical Micelle Concentration of the Ionic Surfactant Sodium Dodecyl Sulfate (SDS) in Aqueous Solution. *J. Phys. Chem. B* **2018**, *122*, 3931−3943.

(15) Shinoda, W.; DeVane, R.; Klein, M. L. Multi-property fitting and parameterization of a coarse grained model for aqueous surfactants. *Mol. Simul.* **2007**, *33*, 27−36.

(16) Shinoda, W.; DeVane, R.; Klein, M. L. Coarse-grained force field for ionic surfactants. *Soft Matter* **2011**, *7*, 6178−6186.

(17) Jalili, S.; Akhavan, M. A coarse-grained molecular dynamics simulation of a sodium dodecyl sulfate micelle in aqueous solution. *Colloids Surf., A* **2009**, *352*, 99−102.

(18) Jusufi, A.; Hynninen, A. P.; Panagiotopoulos, A. Z. Implicit Solvent Models for Micellization of Ionic Surfactants. *J. Phys. Chem. B* **2008**, *112*, 13783−13792.

(19) Wang, S.; Larson, R. G. Coarse-Grained Molecular Dynamics Simulation of Self-Assembly and Surface Adsorption of Ionic Surfactants Using an Implicit Water Model. *Langmuir* **2015**, *31*, 1262−1271.

(20) Hoogerbrugge, P. J.; Koelman, J. M. V. A. Simulating Microscopic Hydrodynamic Phenomena with Dissipative Particle Dynamics. *Europhys. Lett.* **1992**, *19*, 155−160.

(21) Groot, R. D.; Madden, T. J. Dynamic simulation of diblock copolymer microphase separation. *J. Chem. Phys.* **1998**, *108*, 8713−8724.

(22) Koelman, J. M. V. A.; Hoogerbrugge, P. J. Dynamic Simulations of Hard-Sphere Suspensions Under Steady Shear. *Europhys. Lett.* **1993**, *21*, 363−368.
(23) Español, P.; Warren, P. Statistical Mechanics of Dissipative Particle Dynamic. *Europhys. Lett.* **1995**, *30*, 191−196.
(24) Groot, R. D.; Warren, P. Dissipative Particle Dynamics:Bridging the gap between atomistic and mesoscopic simulation. *J. Chem. Phys.* **1997**, *107*, 4423−4435.
(25) Groot, R. D. Mesoscopic Simulation of Polymer-Surfactant Aggregation. *Langmuir* **2000**, *16*, 7493−7502.
(26) Groot, R. D. Applications of Dissipative Particle Dynamics. In *Novel Methods in Soft Matter Simulations*; Karttunen, M.; Lukkarinen, A.; Vattulainen, I., Eds.; Lecture Notes in Physics: Berlin, Heidelberg, 2004; Vol. *640*, pp 5−38.
(27) Groot, R. D.; Rabone, K. L. Mesoscopic Simulation of Cell Membrane Damage, Morphology Change and Rupture of Nonionic Surfactant. *Biophys. J.* **2001**, *81*, 725−736.
(28) http://lammps.sandia.gov.
(29) Chen, Z.; Cheng, X.; Cui, H.; Cheng, P.; Wang, H. Dissipative particle dynamics simulation of the behaviour and mcrostructure of CTAB/octane/1-butanol/water miceroemulsion. *Colloids Surf., A* **2007**, *301*, 437−443. ISSN: 0927-7757. https://www.tib.eu/de/suchen/id/BLSE%3ARN207175560
(30) Mai, Z.; Couallier, E.; Rakib, M.; Rousseau, B. Parameterization of a mesoscopic model for the self-assembly of linear sodium alkyl sulphate. *J. Chem. Phys.* **2014**, *140*, No. 204902.
(31) Mao, R.; Lee, M.; Vishnykov, A.; Neimark, A. V. Modeling Aggregation of Ionic Surfactants using a smeared charge Approximation in Dissipative Particle Simulation. *J. Phys. Chem. B* **2015**, *119*, 11673−11683.
(32) Kekicheff, P.; Gabrielle-Madelmont, C.; Ollivon, M. Phase Diagram of Sodium Dodecyl Sulphate-Water System: 1. A Calorimetric study. *J. Colloid Interface Sci.* **1989**, *131*, 112−132.
(33) Hayter, J. B. A self concistent theory of dressed micelles. *Langmuir* **1992**, *8*, 2873−2876.
(34) Mitra, S.; Karri, R.; Mylapalli, P. K.; Dey, A. B.; Bhattacharya, G.; Roy, G.; Kamil, S. M.; Dhara, S.; Sinha, S. K.; Ghosh, S. K. Reentrant direct hexagonal phases in a lyotropic system of surfactant induced by an ionic liquid. *Liq. Cryst.* **2019**, *46*, 1327−1339.
(35) Li, Y.; Zhang, H.; Wang, Z.; Bao, M. Micelle-vesicle transition in catanionic mixtures of SDS/DTAB induced by salt,temperature,and selective solvents:a dissipative particle dynamics simulation study. *Colloid Polym. Sci.* **2014**, *292*, 2349−2360.
(36) Kim, K. Y.; Byun, K. T.; Kwak, H. Y. The Mesoscopic Simulation on the Structures of the Surfactant Solution Using Dissipative Particle Dynamics. In *ASME International Mechanical Engineering Congress and Exposition*, Proceedings of the International Mechanical Engineering Congress and Exposition (IMECE'2005), 2005; p 80702.
(37) Wu, H.; Xu, J.; He, X.; Zhao, Y.; Wen, H. Mesoscopic simulation of self assembly in surfactant oligomers by dissipative particle dynamics. *Colloids Surf., A* **2006**, *290*, 239−246.
(38) Duan, B.; Zhang, X.; Qiao, B.; Kong, B.; Yang, X. Description of Ionic Surfactant/Water system by Adjusting Mesoscopic Parameters. *J. Phys. Chem. B* **2009**, *113*, 8854−8862.
(39) Lee, M.; Vishnyakov, A.; Neimark, A. V. Calculations of critical micelle concentration by dissipative particle dynamics simulations: The Role of chain Rigidity. *J. Phys. Chem. B* **2013**, *117*, 10304−10314.
(40) Alasiri, H. The Behaviour of Surfactants in Water/ Oil System by Dissipative Particle Dynamics. Ph.D. Thesis, Rice University, 2016.
(41) Lisal, M.; Brennan, J. K.; Bonet Avalos, B. Dissipative particle dynamics as isothermal, isobaric, isoenergetic, and isoenthalpic conditions using Shardlow-like splitting algorithms. *J. Chem. Phys.* **2011**, *135*, No. 204105.
(42) Sanders, S. A.; Sammalkorpi, M.; Panagiotopoulos, A. Z. Atomistic Simulations of Micellization of Sodium Hexyl, Heptyl, Octyl, and Nonyl Sulfates. *J. Phys. Chem. B* **2012**, *116*, 2430−2437.
(43) Bhattacharya, G.; Giri, R. P.; Saxena, H.; Agrawal, V. V.; Gupta, A.; Mukhopadhyay, M. K.; Ghosh, S. K. X-ray Reflectivity Study of the Interaction of an Imidazolium-Based Ionic Liquid with a Soft Supported Lipid Membrane. *Langmuir* **2017**, *33*, 1295−1304.
(44) Herrington, K. L.; Kaler, E. W.; Miller, D. D.; Zasadzinski, J. A.; Chiruvolu, S. Phase Behavior of Aqueous Mixtures of Dodecyltrimethylammonium Bromide (DTAB) and Sodium Dodecyl Sulfate (SDS). *J. Phys. Chem. B.* **1993**, *97*, 13792−13802.
(45) Reiss-Husson, F.; Luzzati, V. The structure of the micellar solutions of some Amphiphilic compounds in pure water as determined by absolute small angle X-ray scattering technique. *J. Phys. Chem. C.* **1964**, *68*, 3504−3511.
(46) Fontell, K. Liquid Crystallinity in Lipid-Water Systems. *Mol. Cryst. Liq. Cryst.* **1981**, *63*, 59−82.
(47) MacKerell, A. D., Jr. Molecular Dynamics Simulation Analysis of a Sodium Dodecyl Sulfate Micelle in Aqueous Solution: Decreased Fluidity of the Micelle Hydrocarbon Interior. *J. Phys. Chem. D.* **1995**, *99*, 1846−1855.
(48) Benrraou, M.; Bales, B. L.; Zana, R. Effect of the nature of the counterion on the properties of anionic surfactants. 1. CMC, ionization degree at the cmc and aggregation number of micelles of sodium, cesium, tetramethylammonium, tetraethylammonium, tetrapropylammonium, and tetrabutylammonium dodecyl sulfates. *J. Phys. Chem. B* **2003**, *107*, 13432−13440.
(49) Moroi, Y.; Nishikido, N.; Uehara, H.; Matuura, R. Interrelationship between heat of micelle formation and critical micelle concentration. *J. Colloid Interface Sci.* **1975**, *50*, 254−264.

https://dx.doi.org/10.1021/acsomega.0c02255
ACS Omega 2020, 5, 22891−22900